CHAPTER 2

INTERACTION OF SELECTED BIOMOLECULES AND METABOLITES WITH AMYLOIDOGENIC PROTEINS*

Abstract

The current chapter focuses on preliminary *in silico* analysis of two amyloidogenic proteins- amyloid β peptide and hen egg-white lysozyme using molecular docking with various intracellular metabolites. As a positive control, some other small molecules were previously reported to have potential anti-amyloidogenic activity. We predicted the aggregation-prone hotspots in these proteins using an online server to specify these molecules' binding sites. We prepared the grid parameter files using this information. Post molecular docking, we analysed the binding energies of these various molecules and their interaction patterns with the aggregation-prone regions of these proteins. Based on our analysis of molecular docking and validating the drug-likeness of these molecules using Lipinski's rule and comparing their binding patterns with the other positive controls, we conclude that nitrogenous bases and selective nucleosides are more suitable to interact with the chosen proteins showing potential anti-aggregation activity. The binding of the molecules could potentially block the amino acid residues within the aggregation-prone zones from interacting, thus blocking self-assembly and intermolecular interactions. The best-selected metabolites included Adenosine, Guanosine (nucleosides), Cytosine, Thymine, Guanine and Uracil (nitrogenous bases). The work provides the foundation for correlating the impact of these metabolites to protein aggregation and misfolding.

---

* Part of the work is published in Kundu, D., Umesh, & Dubey, V.K.* (2020) Interaction of selected biomolecules and metabolites with amyloidogenic proteins, Journal of Biomolecular Structure and Dynamics, 39, 3061-3070.

2.1: Introduction

Amyloidogenesis is an inherent property of all proteins and polypeptide chains, although the degree of propensity varies depending on the protein's primary sequence. Among various factors that lead to protein aggregation, the protein's primary sequence, the conformational state, and the pH of the environment are significant players (Sarkar and Dubey, 2013, Kundu *et al.*, 2020). A proper balance of various intracellular metabolites within the cellular conditions is vital for maintaining an excellent physiological condition. Fully functional biochemical pathways of synthesis and degradation of various metabolites are imperative for maintaining the same. There are reports of various metabolic diseases due to the loss of imbalance of these metabolites. We must also note that most metabolic disorders caused due to the loss of metabolites present with symptoms of neurodegeneration (Fasullo and Endres, 2015). The nucleoside adenosine is reported to act via the A1R and A2R receptors, whose primary function is to release Acetylcholine and glutamate, which changes the level of expressions in advanced stages of AD revealed by post-mortem analysis (Gomes *et al.*, 2011). Studies also report ATP and ADP lowering the Aβ-mediated cytotoxicity at various concentrations. The authors also suggested the role of some critical residues like Tyr^{10} and Ser^{26} with the metabolites through their computational studies (Coskuner and Murray, 2014, Kundu *et al.*, 2020).

We have explored a more comprehensive class of intracellular metabolites in the current chapter, including nitrogenous bases, nucleosides, and dNTPs. The idea was to identify some molecules that show comparable binding affinity with the amyloidogenic regions of these proteins, giving us more clarity into their potential mechanisms compared to other small molecules. Drug discovery and development for protein misfolding diseases are pretty slow for various factors: a) lack of animal models which show complete exhibition of the symptoms of AD and b) lack of biomarkers that could help with the correct determination of the progress of the disease (Beitia-Lakey *et al.*, 2019; Chian & Koo, 2014). Among other previously reported molecules, carotenoids and polyphenols have been identified as potential anti-amyloidogenic molecules having an essential role in progressing neurodegenerative conditions. More recently, various authors have also reported

flavonoids, surfactants and alkaloids as potential anti-aggregation molecules (Feroz *et al*., 2015, Das *et al*., 2018, Maurya *et al*., *al.*, 2015, Sharma *et al.*, 2017, Jash & Kumar, 2014). One of the primary reasons for using HEWL in the current study is that it is known to bind reversibly with various small molecules showing good drug-likeness. This critical feature helps researchers understand various small molecules' transportation and metabolism and the dynamics underlying protein-ligand interactions (Das *et al.*, 2018; Li & Li, 2011).

Hen egg-white lysozyme is a small globular protein of 129 amino acids with six tryptophan residues Trp28, 62, 63, 108, 111 and 123, with a molecular weight of around 14.4kDa. The protein's active site contains a deep cleft, essentially dividing the active site into two halves connected by an α helix. One of the two regions is primarily helical, and the other is composed of β sheets (Das *et al.*, 2018; Strynadka & James, 1991). Tryptophan residues 62, 63 and 108 form a part of the active site of lysozyme and are reported for involvement in substrate binding and inhibition of the enzyme. As a result, small binding molecules to these residues also help stabilise the protein. Another rationale for using HEWL as a model protein other than amyloid β peptide is that it shared high homology (60%) with human lysozyme. Human lysozyme is naturally amyloidogenic, which is involved in systemic amyloidosis non-neuropathic in nature (Booth *et al.* 1997; Khan *et al.* 2014). Lysozyme is a mixed protein with distinctive α helical and β sheet structures. Regions of amino acids 1-36 and 87-129 represent α-helix, and 37-86 form the β sheet region (Khan *et al.* 2014). Amyloid β peptide is the main peptide that is directly implicated in causing aggregates and forming plaques in AD and has been used reportedly for various *in silico* and *in-vitro* studies.

2.2 Methodology

2.2.1 Preparation of model proteins: We chose two model proteins for the current study: hen egg-white lysozyme (PDB ID: 1DPX) and amyloid β peptide (1IYT). We chose the structures based on lower resolution and which had higher relevance for existence under physiological conditions. We downloaded the PDB structures and the respective FASTA sequences from the RCSB database URL rcsb.org (Berman *et al.* 2000). Once we downloaded the structures, we removed water molecules and any other additional small molecules/ions from the basic structure using Pymol

(Kundu *et al.,* 2020). We used SWISS PDB viewer to energy minimise the proteins. After energy minimisation, we submitted the FASTA sequence to CamSol Intrinsic server (https://www-cohsoftware.ch.cam.ac.uk/index.php) is mainly a sequence-based solubility predictor and also predicts aggregation-prone hotspots within the protein. The software predicted two primary aggregation-prone hotspots for amyloid β peptide and five central aggregation-prone regions for hen egg-white lysozyme. The final portion of protein preparation included the addition of charges to the protein, solvation parameters and addition of fragmental volumes to the protein using Autodock Tools 4 (ATD).

Table 2.1- Aggregation-prone regions in hen egg-white lysozyme and grid coordinates for docking

Protein	Grid box No.	Docking Site	Coordinates (X, Y, Z)
HEWL	1	LGNWVCAA (25-32)	-1.176, 19.661, 19.422
	2	YGILQINSR (53-61)	-0.731, 16.786, 19.422
	3	CSALLSSDITASV (80-92)	-0.732, 11.069, 19.422
	4	MNAWVA (105-110)	1.948, 22.902, 20.344
	5	VQAWI (120-124)	-5.571,24.575,16.415
Amyloid β peptide	1	QKLVFFA (15-20)	-0.493, -1.498, -1.043
	2	IIGLMVGGVVIA (31-42)	0.268, 2.392, -13.604

2.2.2 Preparation of Ligands: We retrieved the 3D SDF structure of the various ligands from the Drugbank database and converted them to mol2 format using the PyRx software (Raj *et al.,* 2019). We performed energy minimisation of the ligands using the Conjugate gradient algorithm and Universal force field (UFF). We set the total number of steps of energy minimisation at 200 with an energy difference of 0.1 kcal/mol. We added Kollman charges and Gasteiger charges to minimise proteins and ligands, respectively. Finally, we used the TORSDOF utility in the Autodock Tools to set the ligands' default root, rotatable bonds and torsions.

2.2.3 ADME analysis of ligands: We analysed the physicochemical properties of the ligands using the SWISS ADME server. We listed the physicochemical properties and validated the overall drug-likeness of all the ligands based on Lipinski's rule of five (Diana *et al.,* 2017, Raj *et al.,* 2019).

2.2.4 Molecular Docking using Autodock Tools: Virtual screening of large drug databases is a critical step for drug discovery processes today. Assimilated information about the drug in the database also helps repurpose various FDA-approved drugs for multiple uses. These studies can be sped up using advanced *in silico* techniques like molecular docking, dynamics and simulation. The process also helps in understanding how the drugs could modulate the target. Utilising the broad applicability of molecular docking, we have screened various molecules under the category of nucleosides, nitrogenous bases and dNTPs to elucidate their capacity to interact with the aggregation-prone zones in the chosen model proteins. We utilised a structure-based drug design strategy keeping the target protein rigid and all the ligands flexible for all molecular docking processes. We utilised the Lamarckian Genetic Algorithm (LGA) for the docking process. LGA is considered one of the best docking algorithms compared to other algorithms in Autodock 4 (Morris *et al.* 1996; Huey *et al.* 2007; Venkataesan *et al.* 2012). The algorithm uses a five-term force field-based function called AMBER: the five-term components of the force field include- The Lennard-Jones dispersion term, a directional hydrogen bonding term, a columbic electrostatic potential term, an entropic term and an intermolecular pair-wise desolvation term (Morris *et al.* 1998; Venkataesan *et al.* 2012). We analysed each ligand for a total GA of 20 runs (conformations), and all other parameters were set at default. The initial population size was set at 300 with random starting positions and conformations, and we evaluated a total of 2.5 million energy evaluations (Venkatesan *et al.*, 2012). The positive control for docking purposes included FDA-approved drugs- Donepezil, Galanthamine, Rivastigmine, and other small molecules including Coumarin, Resveratrol, and Curcumin reported earlier to have shown anti-amyloid activity (Beitia *et al.* 2019).

2.2.5 Visualisation and analyses: For general visualisation of the protein models and the protein-ligand complexes, we used Pymol. For analysis of interactions between the protein-ligand complexes, we used the LigPlot+ program (Laskowski and Swindells, 2011), and for analysis of other non-covalent interactions, we used the online platform Protein-Ligand Interaction Profiler (PLIP) (Salentin *et al.* 2015).

3.0 Results

3.1 Docking analysis with hen egg-white lysozyme: The ligands chosen for the current study are small molecules. We have represented the docking interactions and the binding energy with different ligands in different aggregation-prone regions. Some prominent residues of the active site of HEWL include Asp^{52}, Gln^{57}, Asn^{59}, Trp^{62} and Trp^{63}, Ile^{98}, Asp^{101}, Gly^{102}, Asn^{103}, Ala^{107} and Trp^{108}. It is also interesting to note that some active site residues are parts of the various aggregation-prone zones. Our results have shown that most of the test ligands in this study interact with various amino acids in different aggregation-prone regions. The type of interactions between our ligands and amino acids mainly included several hydrogen bonds. Other than conventional hydrogen bonds, non-covalent interactions like salt bridges, pi-alkyl and pi-stacking interactions played a key role. $Tryptophan^{108}$, an essential residue from the structural stability perspective of the protein and a part of the 4th predicted aggregation-prone zone, is one of the critical residues that show strong pi-type interactions. Glu^{35} and Asp^{52} are critical residues involved in salt bridge interactions and form an essential part of the active site. They lie in the close vicinity of the first and the second aggregation-prone region of HEWL. Our results also show that different ligands exhibit different types of interactions in different binding sites, which suggests the versatility of the ligands in their interaction patterns. We also report that this study's chosen set of ligands has a preferential binding for the HEWL active site residues. Besides the protein's active site, the ligands also show a strong binding affinity for residues between the 80th-92nd region and 105^{th}-110^{th}. These are also predicted aggregation-prone regions of HEWL. Hydrophobic interactions also play an essential role in other interactions besides hydrogen bonding. Hydrophobic interactions are a fundamental category for protein-small molecule interactions because they help the protein attain a more stable state of folding in the presence of the ligands. Among other non-covalent interactions, pi-alkyl, pi-cation, and salt bridge interactions also played an essential role in stabilizing protein-ligand interactions. Another key observation from our results was that smaller size compounds like nitrogenous bases and nucleosides had better interaction capability with various regions of HEWL. When we compared the binding energy and the Ki values of our test ligands with that of the FDA-approved

drugs and other small molecules, we found some of our ligands to have better binding energy and Ki values, which suggests that selected molecules out of these set could indeed be taken forward for further studies. We have represented the critical information about the docking in various sites of hen egg-white lysozyme in Table 2.2 to Table 2.6.

Table 2.2-Details of various interactions between the amino acids and ligand when grid box no. 1 **(25-32: LGNWVCAA)** of HEWL. Detailed interaction of top 5 ligands based on binding energy is also given. N/A applies Not Applicable.

Ligand	Binding energy (kcal / mol)	Hydrogen bonds	Non-Covalent Interactions	Hydrophobic interactions	Inhibitor Constant (Ki) µM
GMP	-7.8	Asn46(2), Asn59, Trp62,63, Asn103	Asp52 (Salt Bridge), Trp108 (Pi Stacking)	N/A	1.91
Uridine	-6.16	Ans46, Asp52, Leu56, Asn59, Trp108, Ala107, Val109	N/A	N/A	30.4
Guanine	-6.08	Gln57, Ala107, Val109	Glu35, Asp52 (Salt Bridges)	N/A	34.87
AMP	-5.93	Asn59(2), Trp62,63,108, Ala107,110, Val109	N/A	N/A	45.03
CMP	-5.45	Glu35, Asp52, Asn59, Trp63, Val109, Ala110	N/A	N/A	100.52
Donepezil	-8.29	Asn44, Ala110	Glu35, Asp52 (Salt Bridges)	Asn44, Ile98(2), Ala107, Trp108	0.832
Galantamine	-6.81	Trp63	Trp108 (Pi Stacking), Glu35, Asp52 (Salt Bridges)	Asn59, Val109	10.15
Memantine	-6.97	Asn46, Asp52, Asn59	N/A	Asn59, Val109(2)	7.76
Resveratrol	-5.27	Leu56, Trp63, 108	Trp108 (Pi Stacking)	Ile98, Val109	138.18
Curcumin	-6.83	Thr43(2), Asn44, Glu35	N/A	Phe34, Ser 36, Asn37,39, Gln41, Ala42	9.87
Coumarin	-5.59	Val109	Trp108 (Pi Stacking)	Ile98, Trp108	79.69

Table 2.3- Details of various interactions between the amino acids and ligand when grid box no. 2 **(53-61: YGILQINSR)** of HEWL was fixed for the docking. Detailed interaction of top 5 ligands based on binding energy is also given. N/A applies Not Applicable.

Ligand	Energy (kcal/mol)	Hydrogen bonds	Non-Covalent Interactions	Hydrophobic interactions	Inhibitor Constant (Ki) µM
GMP	-5.27	Glu35, Ser36, Asn37,39, Thr43(2), Asn44(2)	N/A	N/A	1.91
Thymine	-5.18	Ser36, Asn39, Thr43(2), Asn44(2)	N/A	Ile98	160.72
Guanine	-4.84	Gln57, Asn59 (2), Trp63	Asp52 (Salt Bridge), Trp108 (Pi Stacking)	N/A	281.74
TMP	-4.84	Glu35, Thr43(2), Asn44	N/A	N/A	284.2
Uracil	-4.79	Leu56, Trp63, Ala107	N/A	Ile98	306.0
Donepezil	-5.57	Asn39	N/A	Asn 37, 44, Ala 42, Gln 57	84.17
Galantamine	-5.24	Asn37,44	N/A	Ala42	144.55
Memantine	-5.97	Gln57	N/A	Ala42	41.87
Resveratrol	-4.97	Tyr20, Asp101 (2)	N/A	Lys96,97 (2)	228.92
Curcumin	-3.71	Glu35, Asn37, Thr43(2), Asn44	N/A	Asn39, Ala42	1920
Coumarin	-5.14	Glu35, Asn39 (2), Gln41, Asn44	N/A	Ala42	84.92

Table 2.4- Details of various interactions between the amino acids and ligand when grid box no. 3 **(80-92: CSALLSSDITASV)** of HEWL was fixed for the docking. Detailed interaction of top 5 ligands based on binding energy is also given. N/A applies Not Applicable.

Ligand	Energy (kcal/mol)	Hydrogen bonds	Non-covalent interactions	Hydrophobic interactions	Inhibitor Constant (Ki) µM
Guanine	-4.82	Ala82, Ser85, Thr89, Ala90, Ser91	Asp52 (Salt bridge)	N/A	292.21
GMP	-4.5	Ala82(2), Ser85(2),86, Thr89, Ala90	Asp87(Salt Bridge)	N/A	503.18
Cytosine	-4.23	Asp52, Gln57, Asn59, Trp63	Trp108 (Pi stacking)	Trp108	792.07
Thymine	-4.05	Leu56, Asn59, Trp108	Trp108 (Pi stacking)	N/A	174.04
Thymidine	-3.98	Ala82,90, Ser85, Asp87 (2)	N/A	N/A	1200
Donepezil	-5.21			Ile78, Ala82, Asn93	152.84
Galantamine	-3.85	Lys1, Leu84(2), Ser86	N/A	Gln41	1510
Memantine	-4.57	Asp87	N/A	Ala90	445.12
Resveratrol	-4.33	Ser81, Asp87 (2), Ala90	N/A	Ala82, Asp87, Ala90	671.1
Curcumin	-3.15	Gln41, Asp87, Thr89, Ala90	N/A	Ala82, Leu84, Ala90	4900
Coumarin	-5.12	N/A	Lys97	Ile78(3), Ala90	138.61

Table 2.5-Details of various interactions between the amino acids and ligand when grid box no. 4 **(105-110: MNAWVA)** of HEWL was fixed for the docking. Detailed interaction of top 5 ligands based on binding energy is also given. N/A applies Not Applicable.

Ligand	Energy (kcal/mol)	Hydrogen bonds	Non-Covalent Interaction	Hydrophobic interactions	Inhibitor Constant (Ki) µM
GMP	-7.67	Asn46, Ser50 (2) Trp62,63	Glu35, Asp52 (Salt Bridges), Trp108 (Pi stacking)	N/A	2.4
Guanine	-6.05	Gln57, Ala107, Val109	Glu35, Asp52 (Salt Bridges)	N/A	36.65
TMP	-5.71	Glu35, Asp52, Trp62,63,108, Val109, Ala110	N/A	N/A	65.52
AMP	-5.58	Glu35, Asp48, Ser50, Asp52, Asn59, Trp62, 63, Val109, Ala110	N/A	N/A	81.66
Adenosine	-5.34	Glu35, Gln57, Asn59, Trp63, Ala107	N/A	N/A	122.54
Donepezil	-8.15	Trp62, 63	Glu35, Asp52	Asn44, Gln57(2), Trp108, Val109	1.06
Galantamine	-6.87	Trp63	Trp108 (Pi Stacking), Glu35, Asp52 (Salt Bridges)	Asn59, Val109	9.27
Memantine	-6.87	Asn46, Asp52, Asn59	N/A	Asn59, Val109(2)	9.24
Resveratrol	-5.26	Leu56, Trp63, 108	Trp108 (Pi Stacking)	Ile98, Val109, Ala110	139.51
Curcumin	-5.86	Asn46,59, Trp62,63, Ala110	Trp108(Pi Stacking)	Val109	50.31
Coumarin	-5.52	Val109	Trp108 (Pi Stacking)	Ile98(2), Trp108	89.96

Table 2.6- Details of various interactions between the amino acids and ligand when grid box no.5 **(120-124: VQAWI)** of HEWL was fixed for the docking. Detailed interaction of top 5 ligands based on binding energy is also given. N/A applies Not Applicable.

Ligand	Energy (kcal/mol)	Hydrogen bonds	Non-Covalent Interactions	Hydrophobic interactions	Inhibitor Constant (Ki) µM
Thymine	-2.83	Ser24, Gly26, Gln121	N/A	Ile124	8370
Guanine	-2.82	Ser24(2), Leu25	Asp18 (Salt Bridge)	N/A	8530
Uracil	-2.67	Ser24, Gly26, Gln121	N/A	Gln121	11300
Adenine	-2.65	Ser24, Gly26, Asn27, Val120, Gln121	N/A	N/A	11360
Cytosine	-2.52	Asp18, Ser24, Gly26, Leu25	N/A	N/A	14270
Coumarin	-3.49	Leu25, Gly26	N/A	Val120, Gln121	2740
Memantine	-3.86	Asp18, Leu25	N/A	Leu25, Val120, Gln 121(2), Ile124	1450

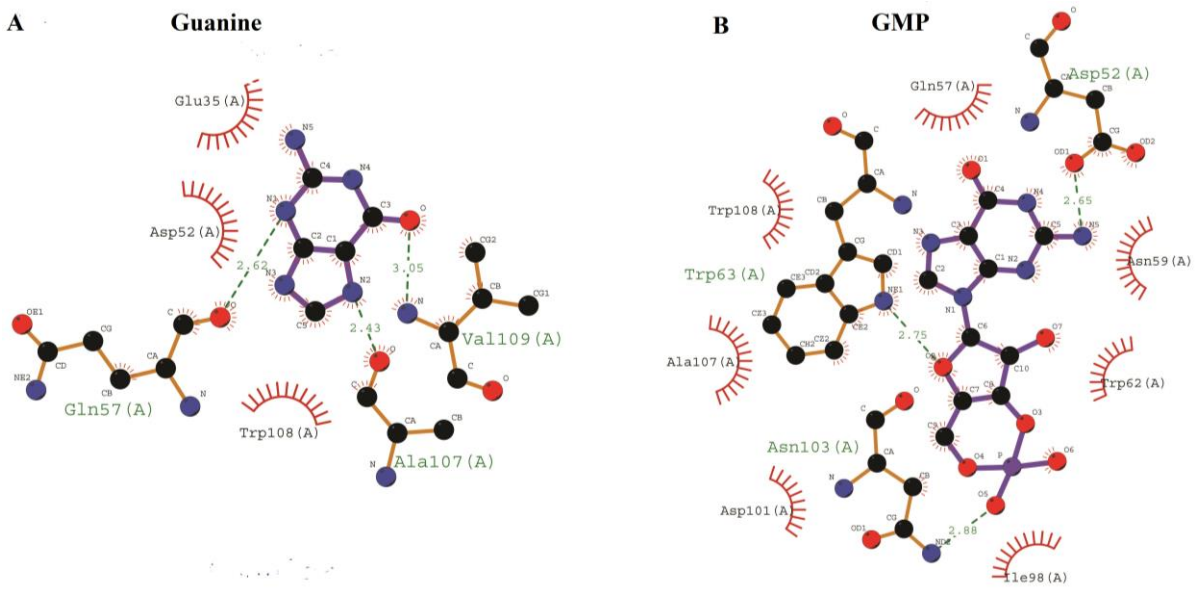

Fig 2.1 Ligplot images showing both hydrogen and hydrophobic interactions: (A) Guanine and **(B)** GMP with aggregation-prone sites of hen egg-white lysozyme. The green dashed lines represent hydrogen bonds with their respective lengths, and the red arcs represent other interactions, viz., hydrophobic interactions

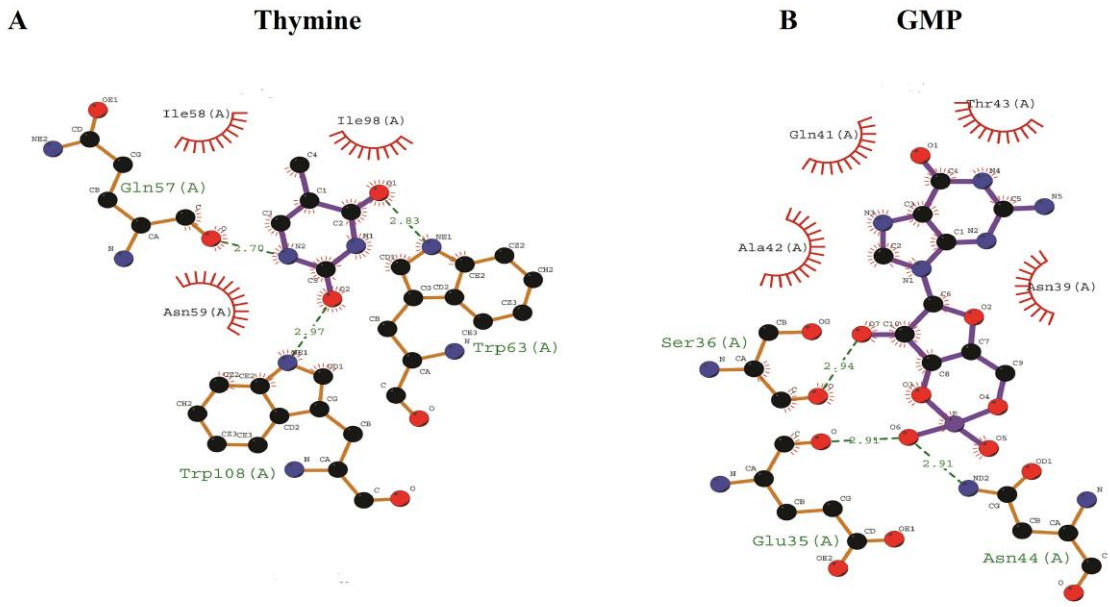

Fig 2.2 Ligplot images showing both hydrogen and hydrophobic interactions: (A) Thymine and **(B)** GMP with second aggregation-prone sites of hen egg-white lysozyme. The green dashed lines represent hydrogen bonds with their respective lengths, and the red arcs represent other interactions, viz., hydrophobic interactions.

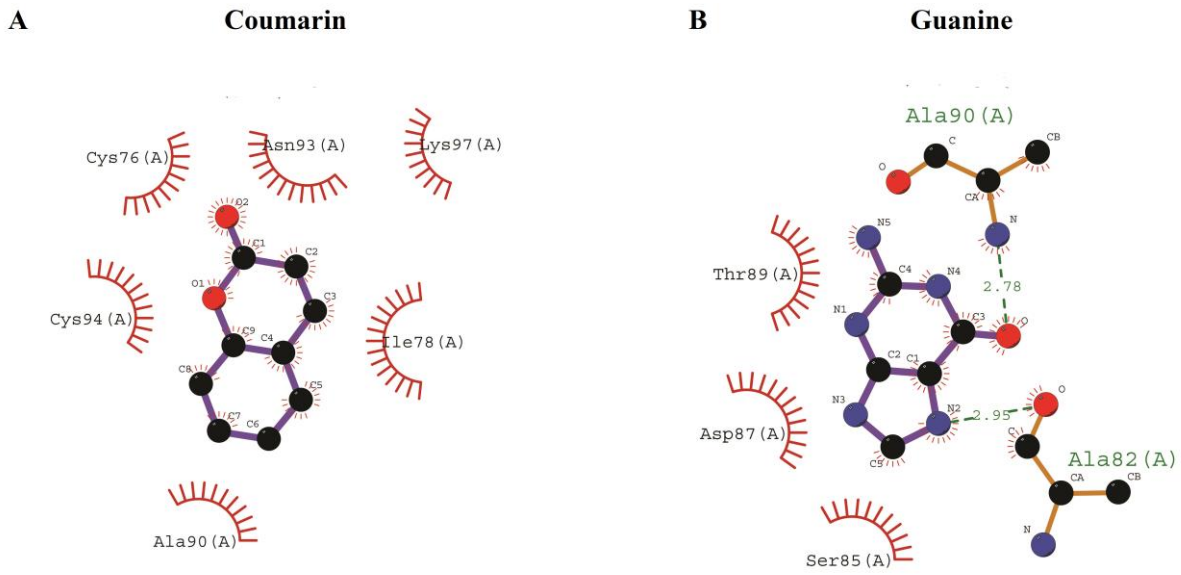

Fig 2.3 Ligplot images showing both hydrogen and hydrophobic interactions: (A) Coumarin and **(B)** Guanine with third aggregation-prone sites of hen egg-white lysozyme. The green dashed lines represent hydrogen bonds with their respective lengths, and the red arcs represent other hydrophobic interactions.

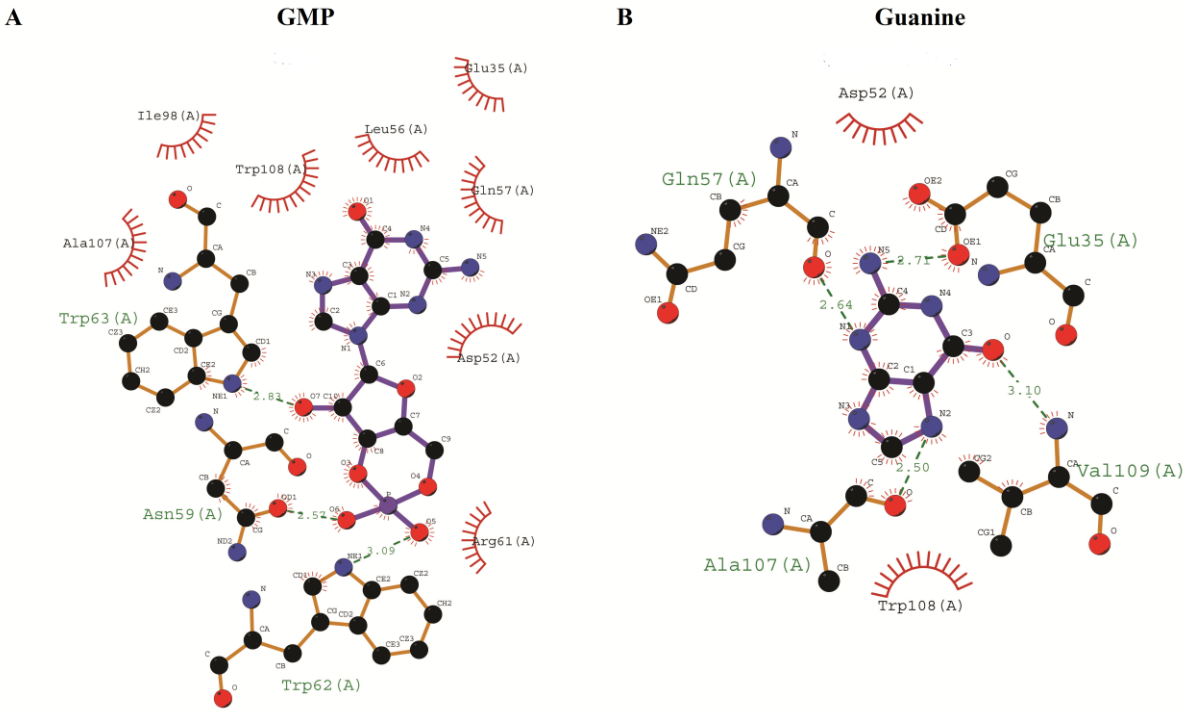

Fig 2.4 Ligplot images showing both hydrogen and hydrophobic interactions: (A) GMP and **(B)** Guanine with aggregation-prone sites of hen egg-white lysozyme. The green dashed lines represent hydrogen bonds with their respective lengths, and the red arcs represent other hydrophobic interactions.

3.2 Docking analysis with Amyloid β peptides: Recent studies on amyloid β peptides have shown an array of structural polymorphisms within the Aβ fibrils. During the AD exhibition, various protofibrillar structures might be present, making it difficult for a particular drug to show suitable actions. The variation and polymorphism within the amyloid β peptide arise from the difference in intra and inter-residue interaction patterns. Classically there are two forms of amyloid β peptide- Aβ-40 and Aβ-42. Studies and reports suggest that Aβ-42 are more toxic than Aβ-40. The cytotoxicity is more in Aβ-42 because it attains a triple-stranded S-shaped anti-parallel β strand, giving it a cylindrical and pore-like structure when it forms fibrils (Beitia *et al.,* 2019). We chose the monomeric form of the Aβ-42 in solution (PDB ID-1IYT) to study the effect of our chosen set of ligands in interacting with two potential aggregation-prone zones within this peptide.

In Amyloid β peptide, there are primarily two amyloidogenic regions- 16^{th}-20^{th} amino acid regions. Previous studies have shown that small molecules or ligands that can bind to this region can inhibit fibril formation. The amino acids in this region are also responsible for the self-association of Aβ peptides into fibrils. Aβ 16-20 form antiparallel β sheets by associating with amino acids 17-21 and 18-22 (Tjernberg *et al.* 1996, Kumar *et al.* 2015; Beitia *et al.* 2019). Some studies which deleted the portion of 16-20^{th} amino acid have also reported no formation of Aβ fibrils (Hetenyi *et al.,* 2002, Beitia *et al.,* 2019). Recent studies on surfactin molecules in docking with amyloid β peptide monomer have also identified Ala21 and Asp23 as critical residues for ligand interaction (Verma *et al.* 2016).

Our results show that small molecules like nitrogenous bases bind more strongly with the peptide's aggregation-prone zones than other positive controls. Among nucleotides show strong binding affinity with lower binding energy in the 16-20 amino acid region. Nucleotides like UMP and GMP have better Ki values than other nucleotides, although they are high molecular weight compounds and fail Lipinksi's rule of five. Smaller molecules like nitrogenous bases do not have much binding affinity for the C terminal region (31-42) amino acid but bind to specific amino acids that play a good role in the fibrillation process. In the 16-20 amino acid region, Lys16, leu17 and

Ala21 emerged as crucial amino acids partnered with the ligands forming hydrogen bonds. Ligands also show hydrophobic interaction with residues such as His13, Leu17, Phe20 and Ala21. Among other non-covalent interactions, salt bridge interactions with Lys16 and pi-stacking interactions with Phe20. Interaction with these key residues might potentially inhibit the Aβ fibril formation. Previous studies have reported that among the C-terminal residues, Gly33, Met35 and Gly37 have a significant role to play in ligand interaction within these regions showing anti-amyloidogenic activity (Battisti *et al*., 2017). Met35 is an essential residue whose interaction with ligands can potentially inhibit fibrillation. Another study has reported that the interaction of surfactin with specific C-terminal residues like Leu34 and other residues Val18, Phe20, Gly25 and Ala21 also destabilises the peptides (Verma *et al.* 2015). This study reports UTP and Memantine to have interactions with Met35. Nucleotides GMP and nucleoside Thymidine shows robust interaction with Lys16, Phe20, and Ala21 binding energies ranging from -3.7 to -4.23 kcal/mol. Molecular docking is a stochastic and robust process whose quality depends on the size of the protein-ligand complex, the individual components and the conformation of the complex, the physicochemical properties of the ligand and the number and type of interactions with respective amino acids (Kitchen *et al.* 2004, Kroemer, 2007 and Verma *et al.* 2016). Binding energies ranging from -5.0 kcal/mol to -14 kcal/mol show suitable ligand binding affinity. However, high free energy does not necessarily impose poor quality of docking, and even ligands with high binding energy can also be chosen as a drug based on their stable complex conformation and desirable bonding of amino acids in the targeted region (Hernandez- Rodriguez *et al.*, 2015, Verma *et al.*, 2016).

Table 2.7- Details of various interactions between the amino acids and ligand when grid box no. 1 **(15-20: QKLVFFA)** of Amyloid β peptide was fixed for the docking. Detailed interaction of top 5 ligands based on binding energy is also given. N/A applies Not Applicable.

Ligand	Energy (kcal/mol)	Hydrogen bonds	Non-Covalent Interactions	Hydrophobic interactions	Inhibitor Constant (Ki) µM
Guanine	-3.87	Phe19, Asp23	Asp23 (Salt Bridge)	N/A	1460
Thymidine	-3.72	Lys16, Leu17, Ala21	N/A	N/A	1860
UMP	-3.21	His13/2, Lys16	Lys16 (Salt Bridge)	N/A	4420
Uridine	-3.15	Lys16, Leu17, Ala21	Phe20 (Pi stacking)	N/A	934.98
Uracil	-3.0	Leu17, Ala21	N/A	Phe20	6300
Donepezil	-4.77	N/A	His13 (Pi Stacking)	His13, Lys16/2, Leu17/3, Phe20	317.1
Galantamine	-4.48	Lys16	Phe20 (Pi Stacking)	Lys16, Leu17, Phe20, Val24	518.78
Memantine	-4.2	Leu17, Ala21	N/A	Lys16, Leu17, Phe20/3	831.49
Resveratrol	-3.45	Lys16	N/A	Leu17, Phe20, Ala21, Val24/2	2980
Curcumin	-3.41	Lys16	N/A	Lya16, Leu17 (2), Phe20	3190
Coumarin	-4.1	N/A	Phe20 (Pi), Lys16 (Salt Bridge)	Lys16, Leu17, Phe20(2)	991.42

Table 2.8- Details of various interactions between the amino acids and ligand when grid box no. 2 **(30-42: IIGLMVGGVVIA)** of Amyloid β peptide was fixed for the docking. Detailed interaction of top 5 ligands based on binding energy is also given. N/A applies Not Applicable.

Ligand	Energy (kcal/mol)	Hydrogen bonds	Non-Covalent Interactions	Hydrophobic interactions	Inhibitor Constant (Ki) µM
GMP	-4.23	Leu17, Phe20, Ala21	Lys16 (Salt Bridge), Phe20 (Pi stacking)	N/A	797.34
Thymidine	-3.7	Lys16, Leu17, Ala21	Phe20 (Pi stacking)		1920
Guanine	-3.35	Lys16/2, Leu17, Ala21	N/A	N/A	3500
Thymine	-3.1	Leu17, Ala21	N/A	Lys16, Phe20	5320
Adenine	-3.04	Glu11, Gln15, Lys16	N/A	N/A	5950
Donepezil	-4.59	N/A	N/A	Ile31, Leu34/2	433.6
Galantamine	-4.18	N/A	N/A	Phe20, Val24/2	867.84
Memantine	-5	Ile41	N/A	Val39	216.66
Resveratrol	-3.33	Ala30, Gly33, Ile34	Phe20 (Pi Stacking)	Val24, Ile34, Leu34/2	3600
Curcumin	-2.96	Ala30, Gly33	N/A	Leu34/2	6790

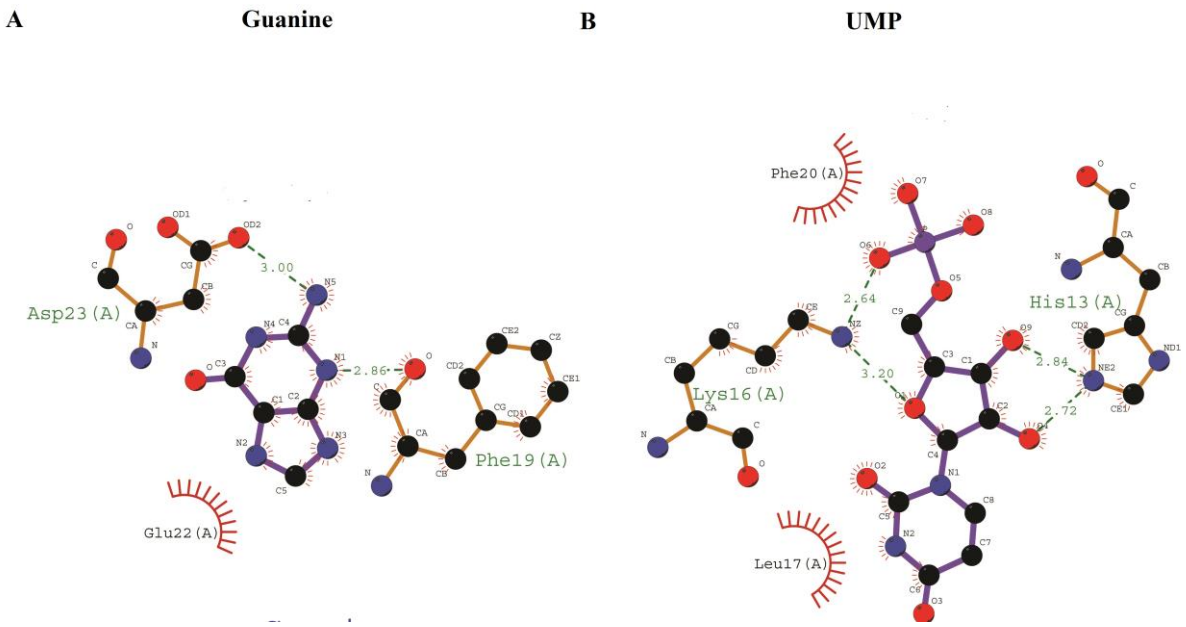

Fig 2.5 Ligplot images showing both hydrogen and hydrophobic interactions: (A) Guanine and **(B)** UMP with first aggregation-prone sites of amyloid β peptide. The green dashed lines represent hydrogen bonds with their respective lengths, and the red arcs represent other hydrophobic interactions.

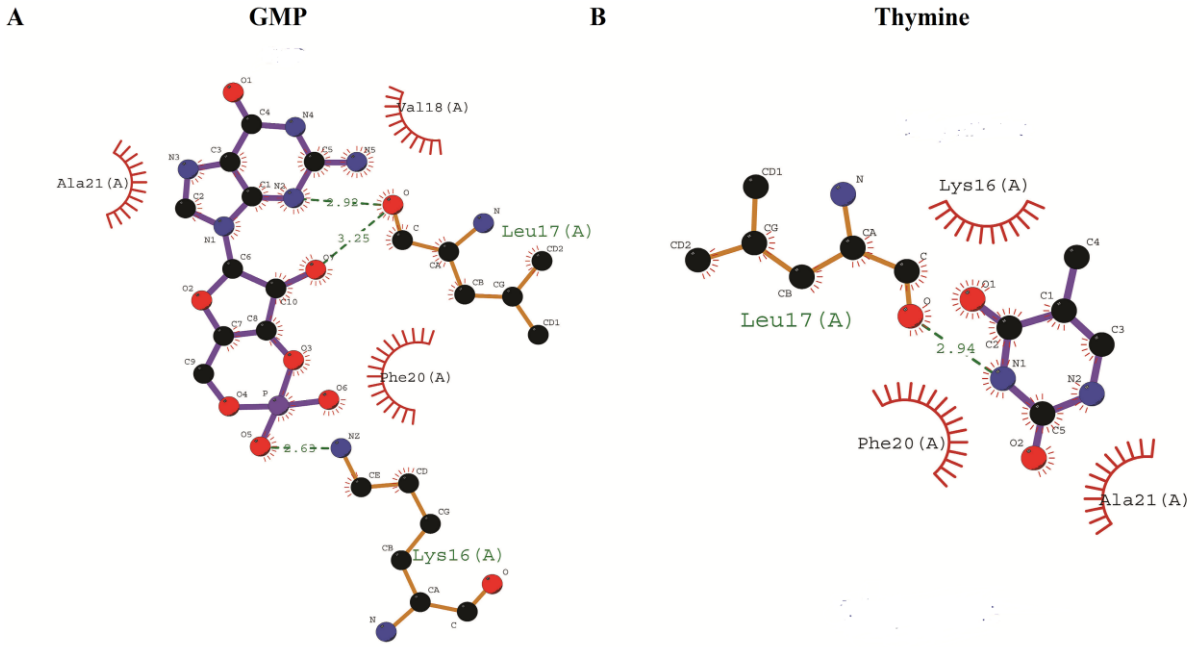

Fig 2.6 Ligplot images showing both hydrogen and hydrophobic interactions: (A) GMP and **(B)** Thymine with aggregation second prone sites of amyloid β peptide. The green dashed lines represent hydrogen bonds with their respective lengths, and the red arcs represent other interactions, viz., hydrophobic interactions.

3.3 SWISS ADME analysis of molecules: Lipinski's rule of five for any small molecule gives us a fair idea about the drug-likeness of any potential drug molecules. Our ADME analysis showed that the chosen set of molecules has a Log P value lower than 0, suggesting that the molecules are more distributed in a hydrophilic environment. Log S values measure the molecule's overall solubility, another critical factor. Our molecules' analyses hint that nitrogenous bases are most suitable for drug molecules. Additionally, nucleoside molecules could be used for experiments, although the final results would depend on experimental analyses. Smaller molecules with good capacity as h-bond donors and acceptors have the highest drug-likeness. The results of the analyses are in Table 9.

Table 2.9- Lipinski's parameters for drug likeliness and ADMET properties of chosen ligands and the approved standard drugs. Log P value represents the lipophilicity of the molecule, Log S value represents the water solubility, TPSA is Total Polar Solvent Accessibility, and BA is the oral bioavailability of a drug.

Molecule	LogP	TPSA (Angstrom)	MW (Da)	H- Donor	H Acceptor	Log S	BA	Lipinski's Rule
Donepezil	3.92	38.77	379.21	0	4	-4.81	0.55	Yes
Galantamine	1.91	41.93	287.35	1	4	-2.93	0.55	Yes
Memantine	2.85	26.02	179.30	1	1	-3.02	0.55	Yes
Rivasgtimine	2.35	32.78	250.34	0	3	-2.69	0.55	Yes
Adenine	-0.2	80.49	135.13	2	3	-1.29	0.55	Yes
Cytosine	-0.58	71.78	111.1	2	2	0.01	0.55	Yes
Guanine	-0.61	100.46	151.13	3	3	-0.71	0.55	Yes
Thymine	0.15	65.72	126.11	2	2	-0.74	0.55	Yes
Uracil	-0.19	65.72	112.09	2	2	-0.42	0.55	Yes
Adenosine	-1.61	139.55	267.25	4	7	-1.05	0.55	Yes
Guanosine	-2.02	159.52	283.24	5	7	-0.61	0.55	Yes
Thymidine	-0.61	124.78	258.23	3	5	-0.73	0.55	Yes
Uridine	-1.62	124.78	244.20	4	6	-0.24	0.55	Yes
Cytidine	-1.85	130.84	243.22	4	6	-0.14	0.55	Yes
ATP	-3.56	308.56	507.18	6	17	0.93	0.11	No
GTP	-4.32	328.53	523.18	8	16	0.85	0.11	No
CTP	-3.95	299.85	483.16	7	15	1.07	0.11	No
TTP	-2.77	273.57	482.17	6	14	0.70	0.11	No
UTP	-3.75	293.80	484.14	7	15	1.20	0.11	No
AMP	-2.57	195.88	347.22	5	10	0.20	0.11	Yes
CMP	-2.60	187.17	323.20	4	9	0.36	0.11	Yes
GMP	-2.81	215.85	363.20	6	10	0.12	0.11	No
TMP	-0.55	129.66	304.19	2	7	-0.87	0.56	Yes
UMP	-2.57	181.12	324.18	5	9	0.49	0.11	Yes
Curcumin	3.03	93.06	368.38	2	6	-3.94	0.55	Yes
Coumarin	1.82	30.21	146.24	0	2	-2.29	0.55	Yes
Resveratrol	2.48	60.69	228.24	3	3	-3.62	0.55	Yes

4.0 Discussion and Conclusion

Drug development against neurodegenerative diseases is a prolonged process because of certain limitations. In this context, a drug repurposing strategy or selection of potential drug molecules which could be easily assessed and used at various stages of disease progression is essential. In the current work, we have explored the potency of intracellular metabolites that have an essential role in various biochemical pathways and whose loss in homeostasis is associated with some proteinopathy conditions. Direct *in silico* studies utilising such molecules have not been attempted before. Literature from the past revealed various other classes of molecules like flavonoids, surfactants, and alkaloids to have anti-amyloidogenic activity in various proteins like hen egg-white lysozyme, amyloid β peptide, transthyretin and so on. The current study reported that selected intracellular metabolites have good interaction capacity with multiple aggregation-prone zones in both the model proteins. Interactions of the metabolites through various hydrogen bonding, hydrophobic, and other non-covalent interactions suggest that these molecules could prevent possible self-assembly of the amino acids via intramolecular interactions. Notably, the metabolites interact with crucial residues of amyloid β peptide-like $Lys^{16, 17}$, Phe^{20} and $Ala^{21,}$ which have earlier been reported to have substantial roles in providing structural stability to amyloid fibrils. Hence, interaction with these residues could intervene with the fibrillation process and exhibit anti-amyloidogenic activity. Similar results in hen egg-white lysozyme suggest that these molecules' anti-amyloidogenic (anti-aggregation) activity could be a common property of these molecules, which is encouraging given that multiple proteins cause various systemic and neuropathic amyloidosis. ADME analysis shows that smaller nitrogenous bases have more drug-like properties than nucleosides or nucleotides and hence are more suitable as anti-aggregator molecules. This preliminary in-silico study needs to be further analysed using other biophysical and *in-vivo* experiments for a better conclusion.